Spatio-temporal gene expression analysis from 3D in situ hybridization images

Welten, M.C.M.

Chapter 4

3D Reconstruction of gene expression patterns in the developing innate immune system of the zebrafish

M.C.M. Welten [1,2], L.F.M. Bertens[1,2(a)], W.M.E.M. Spoor[1,2(b)], A.H.Meijer[2] and F.J. Verbeek[1]

1 Imagery and Media, Leiden Institute of Advanced Computer Science, Leiden University, Niels Bohrweg 1, 2333 CA Leiden, the Netherlands
2 Institute of Biology, Leiden University, Clusius Laboratory, Wassenaarseweg 64, 2333 AL Leiden, The Netherlands

(a and b equally contributed)

Paper in preparation

Case study Early zebrafish development

ABSTRACT

The zebrafish develops both an innate and an adaptive immune system, closely resembling the innate and adaptive immune system of higher vertebrates (mammals and birds). The innate immune system of zebrafish develops already during de first day of embryogenesis. The zebrafish macrophages and granulocytes are essential cell types involved in the innate immune system and show striking similarities with their counterparts in mammals. On the molecular level, marker genes expressed by zebrafish macrophages and granulocytes are found to be homologous to those in mammals. In this study we make a contribution to the existing knowledge by presenting a three dimensional characterization of marker genes of the zebrafish macrophage and granulocyte lineage. In our study we focus on two maker genes, i.e. *l-plastin*, a general marker of leukocytes; and *mpx*, a specific marker of neutrophil granulocytes. The aim of this study was to analyze complete time series. Analysis was accomplished by investigating the number of cells during normal development. We report data from a pilot study that provides a good basis for further experiments. Gene expression patterns were studied in time series of zebrafish embryos, using fluorescent *in situ* hybridisation (FISH), *in situ* hybridization (ISH) and confocal laser scanning microscopy (CLSM). 3D reconstructions of the gene expression patterns were made using 3D reconstruction software. In this manner, distribution of *l-plastin* and *mpx* expressing cells could be presented in a three dimensional matrix. Furthermore, the techniques presented allow an analytical approach to distribution and migratory behavior of single cells.

Keywords: macrophages, neutrophil granulocytes, zebrafish development, fluorescent *in situ* hybridization, time series, 3D reconstruction.

INTRODUCTION

In recent years the zebrafish, *Danio rerio,* has become an increasingly important model system for several reasons: small size, high fecundity and short generation time (Stern and Zon, 2003). The embryos are completely transparent which makes it possible to study developmental processes in vivo, most of which are completed within a few days. Invertebrates like *Drosophila* and *C. elegans* are thoroughly studied in relation to the immune system. These species however, restrict to development of an innate immune system. The zebrafish develops both an innate and an adaptive immune system (Phelps and Neely, 2005), which closely resemble that of mammals. In the phylogenetic sense, the innate immune system is older than the adaptive immune system. The latter evolved after the divergence of invertebrates and vertebrates. The innate immune system provides a broad protection, without previous exposure to pathogens. The innate immune system responds instantaneously to a pathogen whereas the adaptive immune response needs days or weeks to further develop (Kimbrell and Beutler, 2001). Vertebrates exhibit two distinct cell lineages that are involved in the immune system: the myeloid and the lymphoid lineage. Cells from the myeloid cell line, i.e. granulocytes and macrophages, are very important in the innate immune system (Kimbrell and Beutler, 2001). Different types of granulocytes are able to phagocytose foreign material and destruct parasites. Macrophages are able to engulf invading micro-organisms and cellular debris, and also play a role in adaptive immunity (Kimbrell and Beutler, 2001).
Homologues of white blood cell types and marker genes involved in the haematopoiesis and the immune system in higher vertebrates have also been identified in zebrafish (Crowhurst et al. 2002, De Jong and Zon 2005, Herbomel et al.1999, Lieschke et al. 2001). This is one of the reasons that the zebrafish can be employed as a model to study the interaction of the innate as well as the adaptive immnune system with pathogens; and experimental findings can be extrapolated to human.

Hematopoiesis and white blood cells

Haematopoiesis is the process of formation of all blood cell types. In amniotes (birds and mammals), early haematopoiesis starts in an extra-embryonic region: the yolk sac **(**Bennett et al. 2001; Godin and Cumano, 2005)**.** In later embryonic development, haematopoiesis occurs in the aorta-gonad-mesonephros (AGM) region and the fetal liver. An exception can be found in marsupials and monotremes where embryonic haematopoiesis occurs in an intraembryonic region, in the liver (Old and Deane, 2003). In both birds and mammals, adult haematopoiesis takes place in the bone marrow and the thymus (Bennett et al. 2001; Godin and Cumano, 2005). In the amphibian *Xenopus*, early haematopoiesis starts in the intraembryonic antero–ventral region of the embryo. At larval stages, intraembryonic heamatopoiesis occurs in the dorsolateral plate and the liver; extaembryonic haematopoiesis takes place in the ventral blood island (Chen and Turpen 1995; Robb, 1997; Smith et al 2002). In teleosts such as zebrafish, haematopoiesis starts initially in two distant anatomical areas, both being intraembryonic (Herbomel et al. 1999; Rombout et al. 2005). The embryonic zebrafish erythrocytes arise from posterior lateral plate mesoderm forming the intermediate cell mass (ICM) of the trunk, whereas the myeloid cells form in the anterior lateral plate mesoderm beneath the embryonic heart (Herbomel et al. 1999, Willett et al. 1999). Subsequently, like in

mammals, a wave of haematopoiesis starts in the AGM (Murayama et al. 2006, Willett et al. 1999). Recently, a new, transitional haematopoietic location was revealed during larval stages: the caudal haematopoietic tissue (CHT) (Murayama et al.2006). Around 3-4 days of development, cells from the CHT start seeding the kidney and thymus, which remain haematopoietic locations in the adult zebrafish (Murayama et al. 2006, Willett et al. 1999).
In mammals, a common pluripotent haematopoietic stem cell (HSC) gives rise to three progenitors: a lymphoid, a myeloid and an erythroid progenitor. The myeloid progenitor gives rise to four myeloid cell lineages: 1) macrophages and three types of granulocytes i.e. 2) neutrophils, 3) eosinophils and 4) basophils.
In zebrafish, the myeloid progenitor develops into macrophages and two types of granulocytes: the neutrophils (or heterophils) - closely resembling the mammalian neutrophils - and the eosinophils (Bennett et al. 2001, Crowhurst et al. 2002, Lieschke et al. 2001). A summary of zebrafish blood cells is given in Table 1.

Table 1. Overview of blood cell lineages in zebrafish

Haematopoietic stem cell			
Myeloid lineage			Erythroid lineage
Macrophages	Granulocytes		Erythrocytes
	Neutrophils	Eosinophils	

Macrophages and granulocytes in zebrafish
In zebrafish, a macrophage lineage has been identified which is morphologically and functionally similar to its mammalian counterpart (Crowhurst, 2002; Bennett, 2001; Lieschke, 2001). Macrophages are characterized by an agranular cytoplasm which is large compared to the nucleus. The cytoplasm contains cytoplasmic phagosomes, and vacuoles in which phagocytic materials can be found (Crowhurst et al. 2002; Lieschke et al. 2001).
The neutrophil is the most abundant granulocyte cell type in zebrafish, comprising more than 95% of all observed granulocytes (Lieschke et al. 2001). This cell type closely resembles the mammalian neutrophil, though the segmented nuclei of the zebrafish heterophils are divided into 2 or 3 lobes instead of into 5 lobes like the human neutrophils. Another granulocyte cell type is in the literature often referred to as eosinophil (Lieschke et al. 2001; Crowhurst et al. 2002). The morphological appearance of the zebrafish eosinophil differs considerably from the mammalian eosinophil: the zebrafish eosinophil exhibits characteristics of both mammalian eosinophils and basophils (Bennett et al. 2001; Crowhurst et al. 2002). Both cell types contain granules that are filled with enzymes.
In this study we will especially focus on specific marker genes expressed by macrophages and neutrophil granulocytes, since these cell types play a crucial role in the response to inflammation in both zebrafish and mammals.

Macrophage- and granulocyte - specific gene expression

The first marker investigated in this study is *l-plastin* (leucocytosolic plastin). *L-plastin* was shown to be expressed in macrophages (Herbomel et al. 1999) and this gene has subsequently been used as macrophage-specific marker (Liu and Wen 2002, Renshaw et al. 2006). However, partial overlap with *mpx*-expressing cells has also been reported (Bennett et al. 2001) and recent multicolor FISH studies indicated that *l-plastin* is expressed in all leukocytes (Meijer et al., in press). Therefore, *l-plastin* appears to be a general leukocyte marker, although it is possible that expression in macrophages is stronger than in neutrophils at certain developmental stages.

l-plastin is an actin bundling protein. It is a homologue of the leukocyte-specific plastin found in mammals; it is involved in adhesion and activation of macrophages (Herbomel et al.1999, Jones et al. 1998). It is expressed in an early macrophage population when it spreads over the yolk sac as well as in a dispersed axial population of cells in the anterior yolk, in the region of the hatching gland and the pericardium (Crowhurst et al., 2002). At 24 hpf, *l-plastin* expression is found in cells dispersed over the cranial mesenchyme, the body and in the posterior intermediate cell mass (ICM). From 24 up to 60 hpf, *l-plastin* expressing cells start to colonize the cephalic mesenchyme and eventually, brain compartments and retinas. At around 60 hpf the macrophages in the brain compartments undergo a phenotypical transition into early microglia (Herbomel et al.2001) and the expression of *l-plastin* in this cell type decreases. From 60 hpf onwards, the number of *l-plastin* expressing cells in the head diminishes (Herbomel et al.2001).

The second marker we will study is myeloid-specific peroxidase *(mpx)*, expressed by the neutrophil lineage of zebrafish (Clay and Ramakrishnan 2005, Crowhurst et al. 2001, Lieschke et al. 2001, Meijer et al, in press). It is a peroxidase ezyme, stored in the azurophilic granules of the neutrophils and is involved in the primary defense of the cell. It is the zebrafish homologue for mammalian myeloid- specific peroxidase known as *mpo* (Lieschke et al. 2001). Phylogenetic analyses suggest that it may represent an ancestral peroxidase gene (Crowhurst et al, 2002).

3D atlas of zebrafish development

In our research group, a 3D digital atlas of zebrafish development has been developed (Verbeek et al. 2002). Complementary, a zebrafish gene expression database is under construction in which 3D zebrafish gene expression data can be stored and retrieved (Belmamoune and Verbeek, 2006). 3D gene expression patterns are produced using fluorescent *in situ* hybridization (ZebraFISH) (Welten et al.2006); 3D images are obtained by confocal laser scanning microscopy (CLSM). Currently, the dominant group of images in the zebrafish gene expression database is generated using ZebraFISH, but images using GFP can also be stored in the database. The 3D multichannel images are preprocessed for 3D modeling using TDR-3Dbase software (Verbeek et al. 2000). 3D reconstructions of the gene expression patterns are made and mapped on anatomical structures, using the 3D digital atlas of zebrafish development as a reference. To annotate gene expression patterns in relation to the anatomical structures, the 3D reconstructions are compared with corresponding 3D embryos from the 3D atlas of zebrafish development (http://bio-imaging.liacs.nl/atlasbrowserstart.html).

In this study we present an analysis of two marker genes expressed in macrophages and neutrophil granulocytes during zebrafish development: *l-plastin* and *mpx*, respectively. Three dimensional gene expression patterns in developmental time series of whole mount zebrafish embryos were generated by fluorescent *in situ* hybridization (Welten et al.2006). As an initial study for future research, the spatiotemporal distribution of *mpx* and *l-plastin* expressing cells was characterized during normal development. The visualization of gene expression in 3D, the analysis of cell numbers during normal development, and the gene expression analysis from developmental time series will contribute to a better understanding of the innate immune system in zebrafish and facilitate further analytical studies in the future.

MATERIALS AND METHODS

Embryo collection and in situ hybridization
Zebrafish were kept under standard conditions (www.zfin.org) in our facility. Embryos were staged according to Kimmel et al. (1995), fixed in 4% paraformaldehyde and processed for fluorescent *in situ* hybridization (FISH) (Welten et al. 2006).
In situ hybridization (ISH, Thisse et al. 1993 and 2004) was performed in parallel, as a control for the FISH procedure.

Probe synthesis
cDNA clones for *l-plastin* (BC 062381) and *mpx* (BC056287) were obtained from RZPD (Berlin, Germany) and linearized with EcoRI and BamHI respectively. Digoxigenin-labeled antisense RNA probes were synthesized from linearized cDNA clones, using T7 RNA polymerase (Maxiscript kit, Ambion) following the manufacturer's instructions.

Microscopy and imaging
For embryos stained using our ZebraFISH protocol, microscopy and imaging were carried out as previously described. Confocal images were acquired according to a standard protocol (Welten et al., 2006), using a Leica TCS/SP DM IRBE confocal laser scanning microscope (inverted setup) equipped with an Ar/Kr laser. Excitation of the used fluorophores (Cy3 and SYTOXGreen) resulted in a red and a green channel. All images were obtained with a 5x and a 10 x plan apo lens with a large working distance (NA 0.24). For every image, photo multiplying tube (PMT) gain and offset were averaged to optimise the signal to noise ratio. Images were saved as multi-channel TIFF files. Z-projections of the TIFF images were made using SCIL Image.
Images of NBT/BCIP-stained embryos were acquired using a Leica MZFL-III12 stereomicroscope equipped with a Leica DC 500 digital camera. From a single embryo images were made in different focal planes using Adobe Photoshop image processing software; composite images were made from these images.

Analysis of gene expression patterns
In order to observe the distribution of *mpx* and *l-plastin* expressing cells in relation to heart development, vascularization and haematopoietic events over total embryos, *mpx* and *l-plastin* expressing cells, the body of the embryo was subdived into 1) yolk, 2) tail

(caudal from the yolk extension) and 3) head and trunk. These subdivisions are depicted in Fig.1.

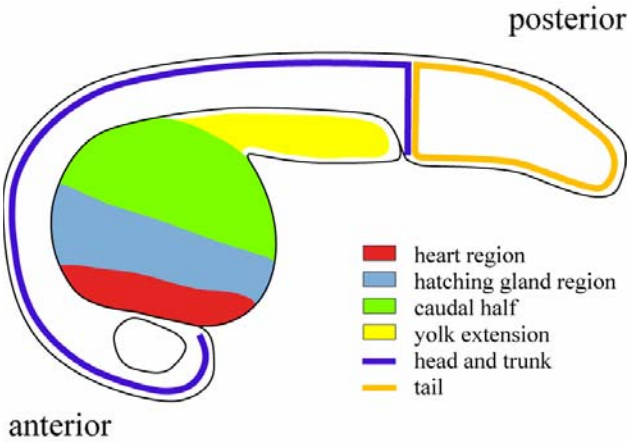

Fig.1 Author's impression of a 24 hpf zebrafish embryo. Overview of regions in the zebrafish embryo, as used for the analysis of cell numbers. In every region, cells were counted in subsequent stages of development.

On the yolk itself, several important vascularization events occur. To investigate the distribution of *mpx* and *l-plastin* expressing cells in relation to haematopoietic events and development of vessels in the yolk region, the yolk was also subdivided. The cells were also counted over four subdivisions of the yolk: 1) heart region, 2) hatching gland region, 3) caudal region of yolk sac, and 4) yolk extension (Fig.1).
From the projections of CLSM images (cf *microscopy and imaging*) as well as from composite light microscopy images from 24 hpf up to 72 hpf embryos, *mpx* and *l-plastin* expressing cells were counted in the subdivisions of 1) the total embryo and 2) the yolk and processed with Excel software. For *mpx*, n = 3-6 embryos and for *l-plastin* n= 3-4 embryos were analyzed. In the analysis, percentages of expressing cells over the above mentioned regions of the total embryos were calculated for all stages. Trendlines were added to demonstrate shifts in cell numbers in certain subdivisions.

3D reconstructions
The multichannel 3D images generated with confocal laser scanning microscopy, were prepared with Scil Image and imported into TDR-3Dbase. 3D reconstructions were made using TDR-3Dbase (http://bio-imaging.liacs.nl/tdr3dbase.html#). Anatomical structures and gene expression patterns were delineated, using TDR-3Dbase and a Wacom LCD graphical tablet.

RESULTS

l-plastin gene expression patterns
In zebrafish, the blood circulation starts at approximately 28 hpf. At this stage, the blood stream flows freely over the yolk sac in the duct of Cuvier, i.e. the future common cardinal vein (Herbomel et al. 1999; Isogai et al. 2001). In our study, the majority of *l-*

plastin expressing cells were indeed found on the yolk at 24 hpf; confirming this important event in blood formation and circulation. From 36 hpf onwards, an increasing number of *l-plastin* expressing cells was found in the head, as visible from the trendline in Fig. 2A. Herbomel et al.(2001) describe migration of macrophages into head mesenchyme and brain structures, and a phenotypical transformation of these macrophages into early microglia at around 60 hpf**.** Indeed, our analysis shows that from 60 hpf onwards, the number of *l-plastin* expressing cells in the head starts to decrease. In 72 hpf embryos, *l-plastin* expression is found in the head, ventrally from the optic cup, and in the anterior part of the trunk. The amount of cells expressing *l-plastin* in the tail increased, as visible from the trend lines in Fig. 2A. On the yolk, the trend lines portray a shift in distribution from the hatching gland region towards the heart region from 36 hpf up to 72 hpf (Fig.2B). This can be explained by the development of the common cardinal veins, which also develop into a more cranial position during these stages (Isogai et al. 2001) and to the regression of the yolk sac from 72 hpf onwards (Herbomel et al.2001).
In Fig. 3 A-E, *l-plastin* expression is shown in a developmental time series of zebrafish embryos at 24, 36, 48 and 60 hpf. At 96 hpf, only few *l-plastin* expressing cells were found in the head. In the tail, though expression was weak in all observed embryos, a string-like pattern of *l-plastin* expressing cells was seen in the ventral part. This is in agreement with the caudal haematopoietic tissue (CHT) described by Murayama et al. (2006). Expression was also found in the dorsal longitudinal anastomotic vessels, as shown in Fig.5A. No expression was seen in the intersegmental vessels.
3D reconstruction for *l-plastin* gene expression at 36 hpf confirms *l-plastin* expressing cells in the head and in the region of the presumptive heart (Fig. 6A and B). 3D reconstruction of a 60 hpf embryo confirms *l-plastin* gene expression inside brain divisions, mainly in the optic tectum and on the roof of the 4th ventricle (Fig. 6 C and D).

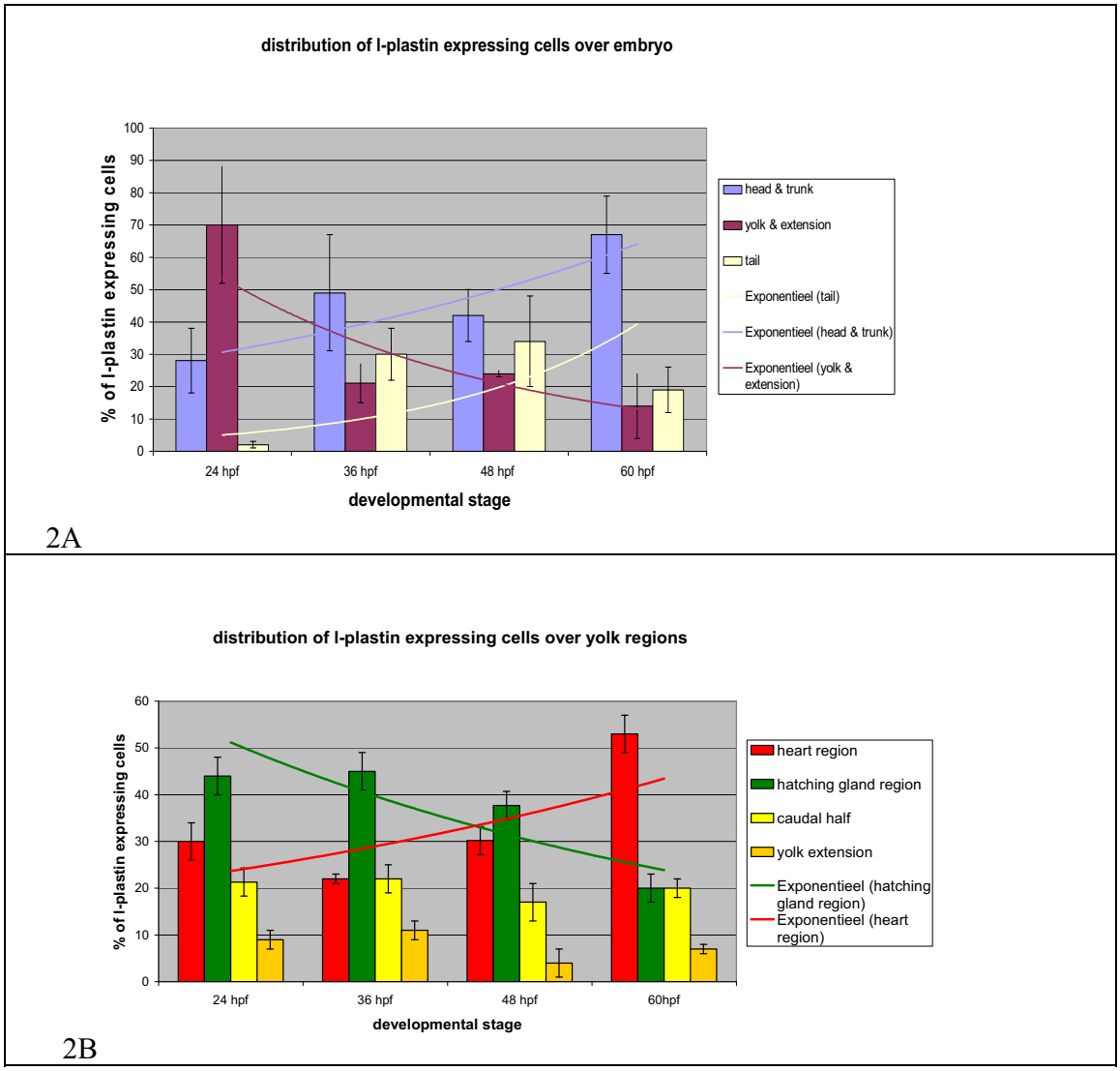

Fig.2. A: Distribution of *l-plastin* expressing cells over the whole embryo (upper panel). The trendlines show an increasing number of *l-plastin* expressing cells in the head up to 60 hpf and in the tail, and decreasing number on the yolk. Lower panel: distribution of *l-plastin* expressing cells over different yolk regions. The trendlines are added to support the idea that an increasing number of *l-plastin* expressing cells can be found in the heart region over time.

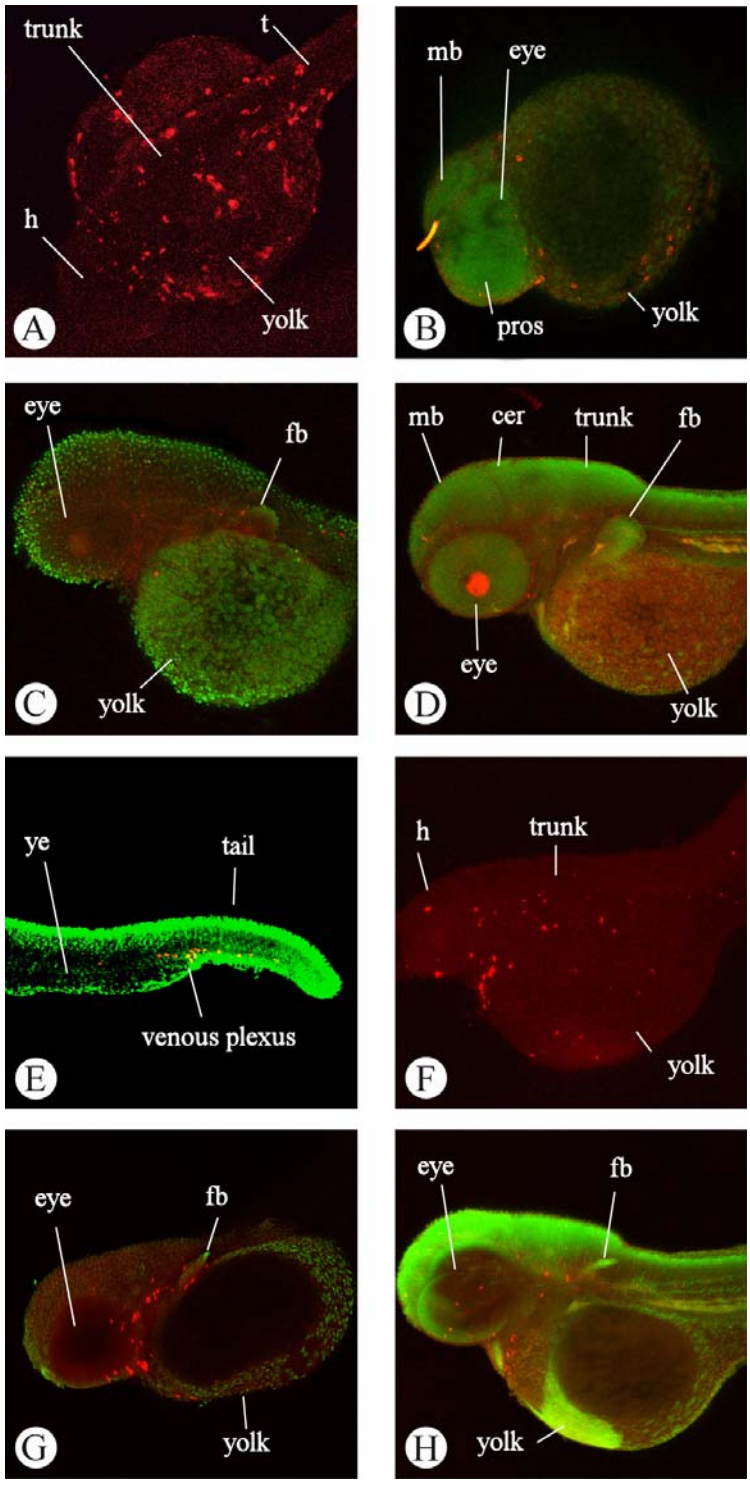
trunk
t
h
yolk
A
mb
eye
pros
yolk
B
eye
fb
yolk
C
mb
cer
trunk
fb
eye
yolk
D
ye
tail
venous plexus
E
h
trunk
yolk
F
eye
fb
yolk
G
eye
fb
yolk
H

Fig. 3

Fig. 3. Panels A-D: developmental series of *l-plastin* expression in zebrafish embryos at 24, 36, 48 and 60 hpf.
Panels E-H: developmental series of *mpx* expression at 24, 36, 48 and 72 hpf. TSA detection.
A is a dorsal view, anterior is to the left; B-H: Anterior is to the left, dorsal to the top. Images are so-called z-projections of confocal images. Gene expression is in red (TSA signal), counterstaining is in green (SYTOX Green).
Abbreviations: cer: cerebellum; fb: fin bud; h: head; mb: midbrain; pros: prosencephalon; t: tail; ye: yolk extension.

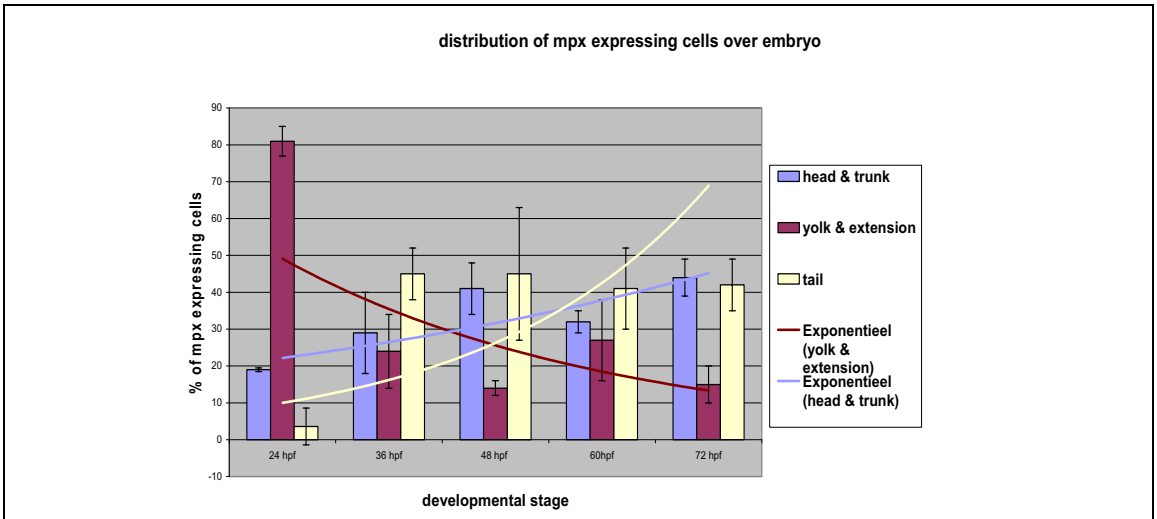

4A

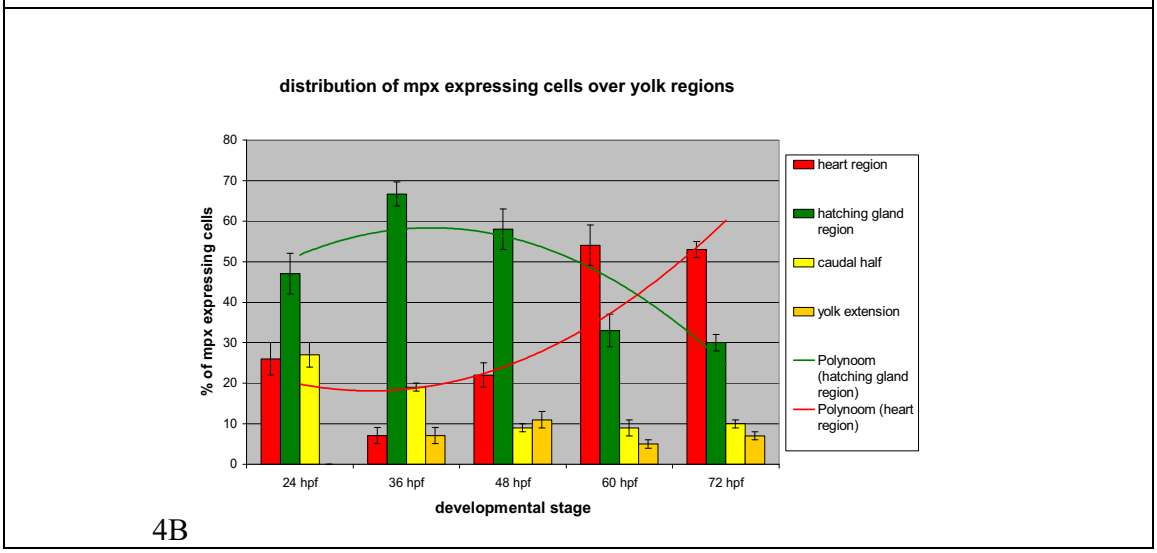

4B

Fig. 4 A: Distribution of *mpx* expressing cells over total embryo; the trendlines show increasing numbers of *mpx* expressing cells in head and trunk, and decreasing numbers on the yolk. B: the distribution of *mpx* expressing cells over different yolk regions. The trendlines are added to support the idea that a shift *in mpx* expression can be observed towards the yolk region adjacent to the heart.

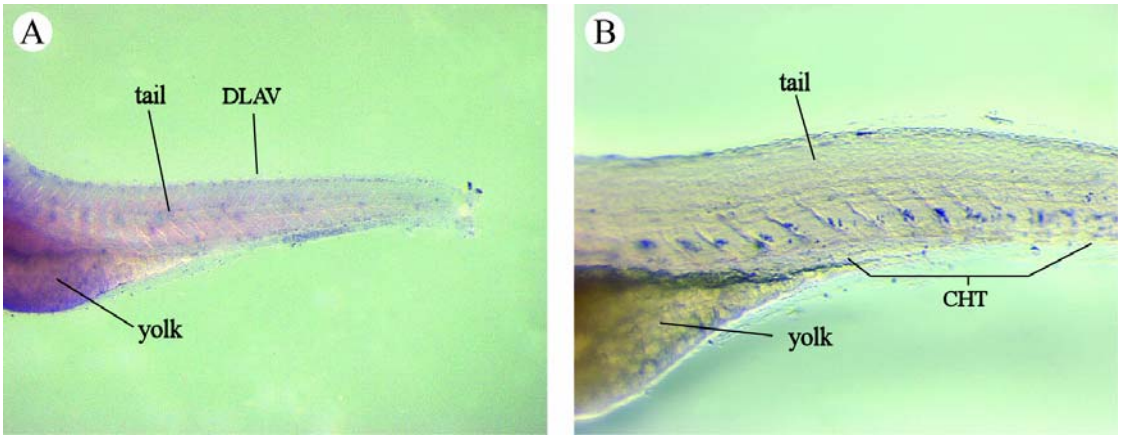

Fig. 5. A: *l-plastin* expression in the tail of a 96 hpf embryo in the dorsal longitudinal anastomotic vessels. B: *mpx* expression in the tail of a 96 hpf embryo. Notice the clusters of cells in the spaces between the somites, as a part of the CHT (Murayama et al. 2006). ISH detection with AP staining. Anterior is to the left, dorsal to the top.
DLAV: dorsal longitudinal anastomotic vessels; CHT: caudal haematopoietic tissue.

Mpx gene expression patterns

A large number of *mpx* expressing cells is found on the yolk at 24 and 36 hpf, in the same pattern as described for the *l-plastin* expression pattern. This is consistent with the onset of circulation at 24 hpf and the pattern of the duct of Cuvier at these stages (Isogai et al.2001). In Fig3 E-H, *mpx* expression is shown in developmental time series at 24, 36, 48 and 72 hpf. From 36 hpf onwards, the number of *mpx* expressing cells on the yolk decreases.

The trend lines suggest a migratory pattern towards the head and trunk (Fig. 4A and 4B), closely following the pattern of vascularization (Isogai et al. 2001) and the development of the heart. At 48 hpf the majority of *mpx* expressing cells is found in the head region and in the tail. At 60 and 72 hpf, expression is found in the head, the tail, the caudal veins and also in the region described as the caudal haematopoietic tissue (Murayama et al. 2006).

At 96 hpf, throughout almost all of the trunk and tail small clusters of *mpx* expressing cells were found in the spaces between the somites on the ventral side of the notochord, forming a part of the CHT (Murayama et al. 2006) (Fig.5B).

Some *mpx* expressing cells were also seen in the caudal vein and dorsal to the spinal cord, in the dorsal longitudinal anastomotic vessels, connected to the intersegmental vessels (Isogai et al. 2001). Scattered *mpx* expressing cells were found in the posterior part of the head and in the heart cavity, as well as in the trunk.

3D reconstruction for *mpx* gene expression patterns portrays *mpx* expressing cells in the common cardinal vein at 48 hpf (Fig. 6 E and F). 3D reconstruction of a 72 hpf embryo depicts *mpx* gene expression in the tail (Fig. 6 G). In the tail, *mpx* expressing cells are visible in the CHT (Fig. 6H).

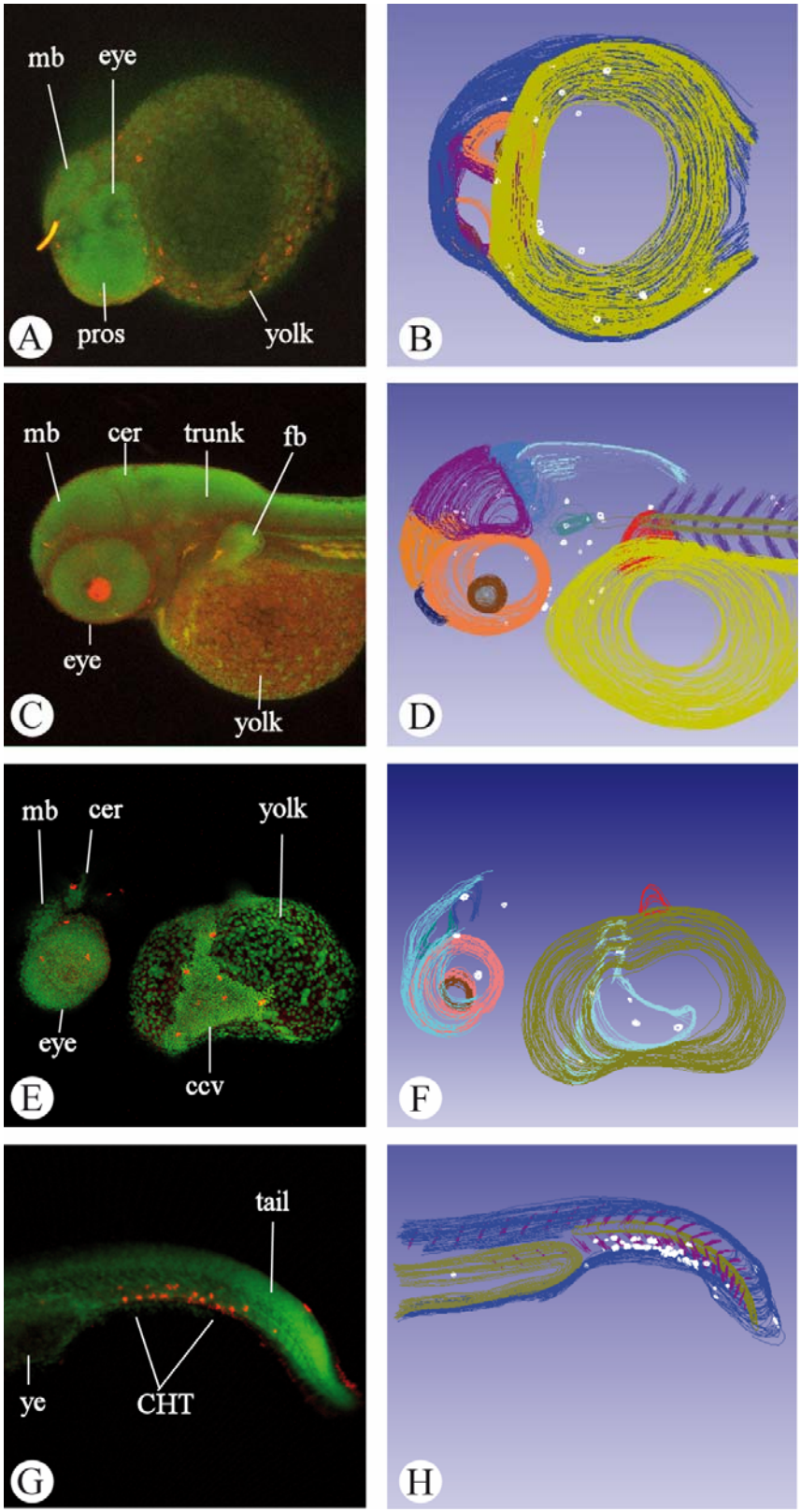
mb
eye
A
pros
yolk
B
mb
cer
trunk
fb
eye
C
yolk
D
mb
cer
yolk
eye
E
ccv
F
tail
ye
CHT
G
H

Fig. 6

Fig.6. A-D: *l-plastin* gene expression at 36 hpf (panel A and B) and at 60 hpf (panel C and D), In panel B and D, the 3D reconstructions of the embryos in panel A and C are depicted. The 3D reconstruction in panel B is magnified and slightly rotated.

E: *mpx* expression in a 48 hpf embryo. F: 3D reconstruction of the same embryo, depicting *mpx* expressing cells in the common cardinal vein i.e. the light blue structure on the yolk (ochre), visible from the confocal image as well as in the 3D reconstruction.
G: *mpx* expression in the tail of a 72 hpf embryo. H: 3D reconstruction of the same embryo, portraying *mpx* expressing cells in the CHT.
The images of the embryos in panel A, C, E and G are the result of TSA detection; The images are so-called z-projections of a confocal image stack. Gene expression is in red (TSA signal), counter staining is in green (SYTOX Green signal). Anterior is to the left, dorsal to the top.

Color legend for the 3D reconstructions in panel B, D, F and H:

l-plastin or *mpx* positive cells (white). embryo outline (dark blue), diencephalon (orange), yolk and yolk extension (ochre), mesencephalon (purple) optic cup (salmon), pectoral fin (red).

Abbreviations: ccv: common cardinal vein; cer: cerebellum; CHT: caudal haematopoietic tissue; fb: fin bud; h: head; mb: midbrain; pros: prosencephalon; t: tail; ye: yolk extension.

DISCUSSION

Gene expression patterns

In our study, the developmental series, cell number analysis and 3D reconstructions portray an increase of *l-plastin* expressing cells in the head up to 60 hpf (Fig.2). From that stage onwards, the number of *l-plastin* expressing cells decreased and at 96 hpf, only a few *l-plastin* expressing cells were found in the head. Herbomel et al. (2001) describe a migration pattern of macrophages from 22 hpf onwards, towards the head mesenchyme. The macrophages then start to colonize brain compartments and the retina. By 60 hpf, the number of *l-plastin* expressing cells in the head signal starts to diminish. The macrophages present in brain and retina undergo a phenotypical transformation into microglia; this is also demonstrated by expression of a marker for the neurotrophic factor *apolipoprotein E* in these cells at 72 hpf (Herbomel et al. 2001).
Between 24 and 60 hpf, by ISH and FISH experiments 20 - 160 *l-plastin* and *mpx* positive cells were detectable on the yolk; 20 - 180 were detectable in the head and 5 - 40 in the tail (Herbomel et al. 1999, Herbomel et al. 2001, this study). However, the total amount detected per embryo showed large variation in our study, probably due to differences in detection sensitivity between experiments. For comparative analysis, we therefore decided to express data as percentages of total cell numbers in different areas. For some developmental stages, only a few datasets were available for analysis. Therefore, the spatio-temporal analysis of distribution of *mpx* and *l-plastin* expression should be considered as a pilot study for future analysis.
Since our study focuses on whole mount FISH and ISH, it has not been not possible to investigate migration of cells over time. However, studies by Herbomel et al. (1999,

2001) and Murayama et al. (2006) demonstrate that both macrophages and granulocytes exhibit migratory behavior as well as cell proliferation.

3D reconstructions
With the confocal microscope settings used in this study, only a limited number of optical sections can be made. Therefore, 3D reconstruction is based on only a part of the embryo. Observations from the 3D models of both *l-plastin* and *mpx* gene expression from 24 hpf up to 72 hpf, are consistent with the gene expression patterns described in literature. In addition, the schematic 3D modeling also allows better inspection of the distribution of the single *l-plastin* and *mpx* expressing cells, and their relation to anatomical structures.

Conclusions and future work
In this study we present 3D gene expression patterns for *mpx* and *l-plastin*. Spatiotemporal gene expression patterns are depicted in developmental time series of zebrafish embryos, and further characterized in 3D models. Exploratory experiments were performed to demonstrate the spatial and temporal distribution of neutrophils and macrophages during development. Both the semi-quantitative data and the 3D reconstructions provide a contribution to the existing knowledge.
In future research, the use of multi-photon microscopy can provide a better depth penetration of the total embryo. Different fluorescent tags will provide the possibility study co-localization of marker genes of leukocytes and other cell types. Eventually, 3D reconstruction of total embryos allows an accurate analysis of cell numbers and distribution in timing series of whole mount embryos, in future functional studies such as inflammation and wounding experiments. The techniques demonstrated in this study, will further facilitate the application of zebrafish as a model to investigate the human immune system.

ACKNOWLEDGEMENTS

This project is supported by The Netherlands Research Council through the BioMolecular Informatics programme of Chemical Sciences (grant number # 050.50.213). We thank G.E.M. Lamers for her valuable advice on confocal microscopy and M. Brittijn for his help with the preparation of the graphical layout of the figures.